Structure and Segmental Motions in Symmetrically Substituted Poly(ferrocenylsilanes): A Carbon-13 CPMAS NMR Contact Time Study

John Rasburn,[†,#] Fazila Seker,[†,$] Kevin Kulbaba,[†] Philip G. Klein,[§] Ian Manners,[†] G. Julius Vancso,[⊥] and Peter M. Macdonald*[,‡]

Department of Chemistry, University of Toronto, 80 St. George St., Toronto, Ontario, M5S 3H6, Canada; Department of Chemistry, University of Toronto at Mississauga, 3359 Mississauga Rd., Mississauga, Ontario, L5L 1C6, Canada; IRC in Polymer Sciences and Technology, University of Leeds, Woodhouse Lane, Leeds, LS2 9JT, U.K.; and Department of Chemical Technology, University of Twente, Drienerlo Laan 5, AE 7522 NB Enschede, The Netherlands

Received April 20, 2000; Revised Manuscript Received December 20, 2000

ABSTRACT: The structure and thermal behavior of two organometallic polymers, poly(ferrocenyl dimethylsilane) (**I**) and poly(ferrocenyl di-*n*-butylsilane) (**II**), have been examined using a variety of physical characterization methods which reveal differences in their crystalline structures and associated segmental librations. In addition to examination with differential scanning calorimetry and wide-angle X-ray scattering, solid-state ^{13}C NMR spectra were acquired for a wide range of $^{1}H-^{13}C$ contact times. The spectra of **I** at room temperature exhibit two isotropic chemical shifts for the methyl groups, indicating the presence of different environments. The initial cross-polarization (CP) times of crystalline, protonated carbons are interpreted with reference to values found in the literature. The main chains of both polymers were found to be fairly rigid on the time scale of T_{CH}, but the side chains of **II** are very disordered. The relevance of the ^{13}C measurements at room temperature is discussed with regard to a higher temperature transition indicated in the DSC trace of **II**.

Introduction

Poly(ferrocenylsilanes)[1−5] (Figure 1) are an interesting new class of organometallic polymer[1] and have been attracting increasing interest with a view to new possible applications.[2] These are highly unusual polymers having a backbone comprising alternating ferrocenyl moieties and silicon atoms. Although low-molecular-weight samples were synthesized some time ago,[3] interest has been rekindled with a novel synthesis route discovered by Foucher et al.[4a]

This ring-opening polymerization method has provided the means to access high molecular weights,[3] and moreover, its simplicity makes it amenable to a range of substituents, polymerization conditions, and copolymerizations.[1] These polymers exhibit peculiar electrochemical behavior,[1] and other polymers containing ferrocene units have been demonstrated to be effective as biosensors and indicators.[2,6] Closely related ferromagnetic materials have also been studied.[7] Novel micellar structures are formed in solutions of ferrocenylsilane−siloxane block copolymers.[8] Certain poly(ferrocenylsilanes) in the solid state become semiconductors with suitable doping.[1]

This report is concerned with comparing the physical properties of the dimethyl (**I**) and di-*n*-butyl (**II**) poly(ferrocenylsilanes) shown in Figure 1. These two polymers are members of a subfamily of symmetrically substituted polymers with R in the range methyl to *n*-hexyl. Interesting trends arise in terms of physical properties and crystalline structure as the number of methylene segments in the side chains is increased. For example, with respect to their thermal behavior, it has been observed that, for those poly(ferrocenylsilanes) where R is *n*-butyl or *n*-pentyl, additional, small endotherms appear in differential scanning calorimetry (DSC) traces just prior to the final, crystalline melting peak (the latter being confirmed as such by optical microscopy).[4d] Several explanations can be conjectured for this, such as the existence of different polymorphs, segregation of different molecular weight fractions during crystallization, or the existence of mesophases such as liquid, plastic, or conformationally disordered[9] ("condis") crystalline. Notable examples of the latter include polyethylene,[9a] 1,4-*trans*-polybutadiene,[9a,b] and polysilanes.[9c−e]

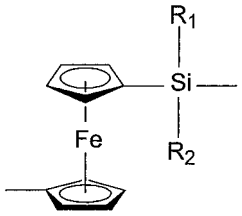

I: $R_1 = R_2 =$ methyl
II: $R_1 = R_2 = n$-butyl

Figure 1. Repeat unit of poly(ferrocenylsilanes) **I** and **II**.

Molecular motions in macromolecules are known to be complex, with a broad range of associated correlation times. For polymers with longer *n*-alkyl side chains there may be additional motions which occur above room temperature. A convenient means of investigating such phenomena involves examining the cross-polarization behavior in cross-polarization, magic angle spinning

[†] University of Toronto.
[‡] University of Toronto at Mississauga.
[§] University of Leeds.
[⊥] University of Twente.
[#] Current address: School of Engineering, University of Exeter, North Park Road, Exeter, EX4 4QF, U.K.
[$] Current address: Polymer Materials Laboratory, General Electric Company, One Research Circle, Niskayuna, NY 12309.
* To whom correspondence should be addressed.

10.1021/ma0006934 CCC: $20.00
Published on Web 04/17/2001

(CPMAS) solid-state ^{13}C NMR experiments,[10,11] which have the additional benefit of yielding optimum conditions for any subsequent ^{13}C NMR measurements. It is also useful to examine the ^{1}H broad-line NMR spectrum,[12,13] which is an essential prerequisite for morphological investigations via ^{1}H NMR diffusion experiments.[14] Deuterium NMR can be employed as well to examine polymer motions,[15] and experiments have been instigated[16] to examine librational motions in poly(ferrocenylsilanes) relative to the glass transition temperature.

This study aims to exploit the capabilities of CPMAS NMR for resolving both different chemical sites and different phases. The ultimate purpose is to provide an estimate for the effective, root-mean-square, heteronuclear dipolar coupling in an approach similar to that of Lauprêtre et al.,[17] who suggested that examination of the signal growth for short cross-polarization times may serve as a convenient alternative to more detailed separated-local-field methods.[18] Comparison of the effective cross-polarization rate with that anticipated for a rigid lattice indicates the extent of motional averaging, provided that the molecular motion taking place is sufficiently fast.[12,13,17c,19] Although cross-polarization dynamics are complex,[20] and the spin dynamics in a powder sample are likely to be heterogeneous,[21] where pronounced differences in librational freedom occur between molecular segments, the initial cross-polarization behavior can be used to identify such differences.

Experimental Section

Synthesis and Sample Preparation. All the poly(ferrocenylsilanes) of the series were synthesized previously as described elsewhere,[4] using thermal ring-opening polymerization of the appropriate [1]-ferrocenophane monomers. Confirmation of high molecular weight[1,3] was by gel permeation chromatography, as described previously (0.1% tetrahydrofuran (THF) solutions with tetra-*n*-butylammonium bromide (0.1%) added),[4b] yielding for **I** M_w = 520K, M_n = 340K, and PDI = 1.5, and for **II** M_w = 890K, M_n = 340K, and PDI = 2.6. The absence of unsubstituted cyclopentadienyl rings in ^{1}H NMR solution spectra (at ca. 3.9 ppm, C_6D_6) also indicates a low concentration of end groups and therefore high molecular weight. To maximize the degree of crystallinity, after purification by repeated precipitations in the standard way, the polymers were allowed to reprecipitate overnight using relatively mild conditions, typically involving 30 mL of a 5% solution in THF diluted dropwise with 150 mL of methanol. Further precipitation was achieved by subsequent addition of more methanol to the mixture. After filtration, the polymer was washed in acetone and dried under vacuum.

Differential Scanning Calorimetry. DSC measurements were carried out on a Perkin-Elmer DSC-7 calorimeter using indium and cyclohexane as standards and with a heating rate of 10 °C min^{-1}.

Wide-Angle X-ray Scattering. Wide-angle X-ray scattering (WAXS) experiments on polymer powder samples employed a Siemens D5000 diffractometer with solid-state detector tuned to the 1.5406 Å (Cu Kα_1) wavelength and reflection geometry. Step-scan mode, reflection geometry, and a step size of 0.1° of scattering angle (2θ) were used, with collection times of 1.0−1.5 s per step.

Solid-State NMR. Solid-state ^{13}C and ^{1}H NMR spectra were obtained at 25 °C on a Chemagnetics CMX 300 spectrometer, operating at 7.00 T. Cross-polarized ^{13}C NMR spectra with magic angle spinning (CPMAS) were acquired using a Chemagnetics MAS probe with a single coil doubly tuned to 299.3 (^{1}H) and 75.3 MHz (^{13}C) with zero offset. Cross-polarization dynamics were determined from standard, single-shot, spin-locked matched transfer sequences,[10,22,23] incorporating appropriate phase cycling.[24] Approximately 100 mg of powdered sample was packed into a 7.5 mm o.d. zirconia rotor and spun at 5 kHz. Hartmann−Hahn matching[25] was optimized for the methyl resonance of hexamethylbenzene (HMB) (132.2 ppm relative to TMS[26]), with rf field strengths of 50 kHz. The ^{1}H rf field was increased slightly to effect matching at the +1 matching sideband.[27] The magic angle setting was monitored using KBr, resulting in a minimum full width at half-height of 75 Hz, i.e., 1.0 ppm, for the aromatic resonance of HMB.[28−30] Spectra were acquired for contact times ranging from 10 μs to 25 ms, using a spectral width of 50 kHz, a recycle delay of 1.0 s, and 2048 data points. For each contact time employed, 600 transients were accumulated (10 min per spectrum). The signal intensities were measured from the peak heights, since the line width of each resonance did not change with contact time.

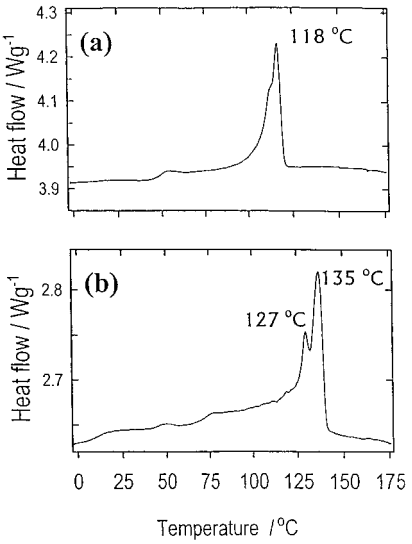

Figure 2. Differential scanning calorimetry traces: (a) **I**; (b) **II**.

Results

Differential Scanning Calorimetry. DSC traces revealing the melting behavior for poly(ferrocenyl dimethylsilane) (**I**) and poly(ferrocenyl di-*n*-butylsilane) (**II**) are shown in Figure 2a and 2b, respectively. **I** exhibits a main melting endotherm at 118 °C, with a poorly resolved and less intense endothermic event evident several degrees lower in temperature. **II** exhibits a main melting endotherm at 135 °C, with an additional, well-resolved endotherm evident at ca. 127 °C. Within the context of the poly(ferrocenylsilane) series having increasing *n*-alkyl side-chain lengths, as listed in Table 1, it is found that the temperature of the main melting transition is highly sample history dependent but that the enthalpy of the main melting transition decreases progressively.

The premelting endotherm evident in the DSC traces in Figure 2 has been observed previously in a study of **I**.[31] Small-angle X-ray scattering measurements[31b] give clear evidence that at this temperature lamellar thickening occurs. Such processes are well-known in other polymers and are contingent on the presence of a conformationally disordered ("condis") state. An alternative explanation is that this endotherm corresponds to the advent of a liquid-crystalline state. However, semicrystalline cast films of **II** show little change under polarizing microscopy over a temperature range spanning the transition temperature. Moreover, molecular weight segregation effects cannot be ruled out given the broad molecular weight distributions in the samples studied.

Table 1. Physical Characteristics of Semicrystalline Di-*n*-alkyl Poly(ferrocenylsilanes)

side chain	T_g[a] (°C)	DSC melting temp[b] (°C)	enthalpy of melting[c] (J g^{-1})	principal WAXS scattering peaks[d] (Å)
hydro[e]	16	165		5.9, 5.1
methyl	33	120	14	6.3, 4.5 (6.7, 6.0)[f]
ethyl	22	100	18	6.6
propyl	24	85	12	10.4, 7.4, 4.7
butyl	3	127, 135	2, 8	17.7, 11.1, 6.4, 4.9
pentyl[g]	−11	84, 102	1, 6	12.2, 6.5, 5.2

[a] Reference 1. Note that the mechanical T_g listed will be higher than the T_g observed by NMR. [b] ±ca. 3 °C (may vary widely according to sample and sample preparation). [c] ±ca. 2 J g^{-1} (references as for a). [d] ±ca. 0.2 Å, expressed in terms of interplanar spacing (ref 1). [e] Reference 4e. [f] Reference 31. [g] DSC analysis on high-molecular-weight cast film.

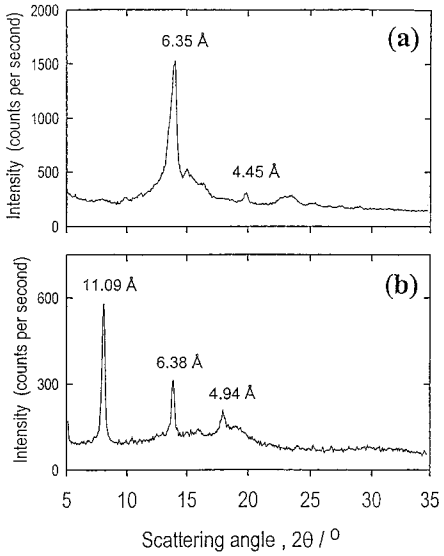

Figure 3. Wide-angle X-ray scattering profiles: (a) **I**; (b) **II**.

Wide-Angle X-ray Scattering. Figure 3 shows WAXS profiles of **I** and **II**. The positions of the principal peaks are listed in Table 1, in terms of the corresponding interplanar spacing. The profile for **I** features a single, broad peak at an interplanar spacing of 6.35 Å (scattering angle of $2\theta = 8°$). The profile for **II** has an intense peak at an interplanar spacing of 11.09 Å (scattering angle of $2\theta = 14°$). The presence of intense, narrow peaks implies crystallite sizes on the order of 100 Å or more. Comparison with the known crystal structure of pentamer of **I**[5] (which has been suggested as a model for the crystal structure for the polymer[5,31a,31d]) indicate that the intense peaks correspond to the spacing between Fe-containing planes[33] and, thus, to the spacing between polymer main chains. From the data in Table 1 it is clear that the effect of increasing side-chain length is to increase the spacing between main chains, as has been seen in other systems.[34] One would anticipate, therefore, that the side chains of **II** would exhibit greater freedom of motion than those of **I**.

^{13}C NMR. Figure 4 shows a series of ^{13}C CPMAS NMR spectra of **I** as a function of the contact time for cross-polarization. The most intense resonance, at approximately 72 ppm, is from the cyclopentadienyl carbons. The three different cyclopentadienyl carbons are not resolved in the spectrum of the solid, in contrast to the situation in solution. The other resonance originates with the methyl side chains and occurs as an asymmetric doublet (2.8 and −1.6 ppm). In solution, the

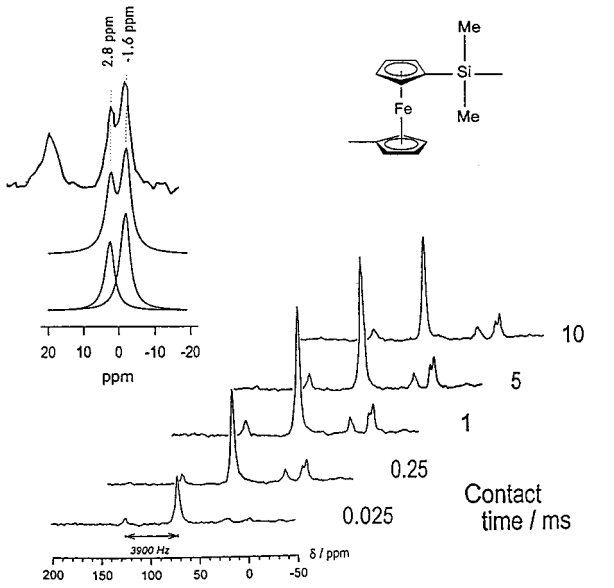

Figure 4. ^{13}C CPMAS NMR spectra at 75.5 MHz and room temperature for poly(ferrocenyl dimethylsilane) (**I**) at selected contact times; the spectra have been modified with 50 Hz of Lorentzian broadening. The inset at the upper left illustrates deconvolution of the methyl resonance into component Lorentzians. The peaks at ca. 125 and 20 ppm are spinning sidebands.

methyl resonance occurs as a singlet positioned at −0.5 ppm.

The detection of this asymmetric methyl doublet suggests the presence of two polymer conformations. Since the doublet is asymmetric, the chemical shift difference between the two resonances cannot be due merely to an inequivalence of the two silicon methyls. Furthermore, the relative intensity of the two components of the doublet is constant as a function of contact time in the cross-polarization experiment (see below). This indicates that the two methyl resonances do not arise simply from two different phases (i.e., crystalline vs amorphous). Specifically, different molecular mobilities in different phases dictate different cross-polarization dynamics, such that at longer contact times more rigid (i.e., crystalline) regions contribute more relative intensity than do more amorphous (i.e., glassy or rubbery) regions. However, the relative intensity is also independent of changes in temperature, which indicates that the observed methyl intensity arises predominantly from crystalline and more glassy amorphous regions in the first place. In this regard, **I** differs markedly from polyethylene, where separate ^{13}C NMR resonances are observed for methylene carbons within amorphous vs crystalline regions of the sample.[13,35]

The precise conformational difference giving rise to the observed methyl splitting is uncertain. One possibility is that "kinks" within the polymer chain produce inequivalent methyl environments. For example, an examination of the crystal structure of the corresponding pentamer,[5] shown in Figure 5a, reveals that the ferrocenyl units at the ends of the chain are oriented differently from those in the interior, being turned through a dihedral angle which places them at approximately right angles to the plane containing the main chain. Barlow et al [36] suggested that this same mixed conformation was likely to occur in the polymer as well. As shown in Figure 5b, the conformation at the chain end produces two different methyl group environ-

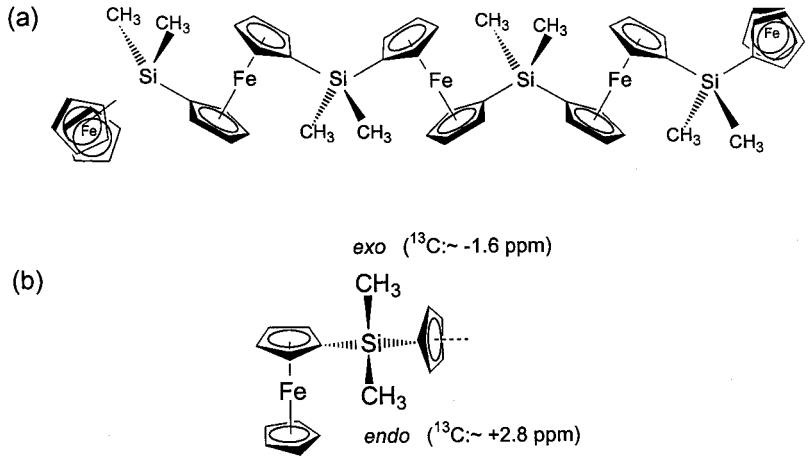

Figure 5. (a) The conformation adopted by the dimethyl pentamer in the crystal structure described in ref 5. (b) Schematic diagram indicating two types of environment for methyl groups in the vicinity of a ferrocenyl group. An argument in the text has it that *exo* is upfield and *endo* downfield from the respective frequencies they would have if no ferrocenyl group was present.

ments: *endo* methyl groups located in a position approximately equidistant from the iron atoms in the two neighboring ferrocenyl units and, conversely, *exo* methyl groups situated more distant from the iron atom in one neighboring ferrocenyl unit than the other. By comparison, all methyl groups within the interior of the chain lie approximately equidistant from either neighboring iron atom. We conjecture that *exo* methyls are deshielded relative to both *endo* and interior methyls, based on their proximity to the deshielding zones of the aromatic cyclopentadienyl rings.[37,38] Consistent with this interpretation is the fact that in solution, where the observed chemical shift represents a weighted average of those corresponding to the chief conformational minima, the methyl resonance occurs at −0.53 ppm, intermediate to the two solid-state values. On the other hand, to produce the observed intensities of the methyl doublet the proportion of kinks would have to be rather high.

Another possible source of the methyl doublets would be the presence of two coexisting crystalline polymer forms. Recent X-ray diffraction studies[39] on poly(ferrocenyldimethylsilanes) indicate that 3D crystalline phases coexist with 2D mesophases having different packing.

To examine this question more closely, we produced amorphous and crystalline samples of **I**. The amorphous sample was prepared by simply precipitating **I** from concentrated THF into hexanes, followed by drying to remove residual solvent. The crystalline sample was prepared by thermal annealing **I** for 5 days at 90 °C under nitrogen and yielded a sharp WAXS *d* spacing of 6.2 Å. ^{13}C CPMAS NMR of the amorphous sample showed only a broad resonance stretching from 0 to 4.0 ppm in the methyl region of the spectrum. The crystalline sample showed a methyl doublet with two well-resolved methyl resonances at the same positions described above. However, the intensities of the two resonances were now roughly equal. Evidently, the resolution and intensities of the two methyl resonances are sample history dependent. This might prove a useful means of sample characterization and is worthy of a fuller investigation.

Figure 6 shows the CPMAS ^{13}C NMR spectrum of **II**. All the expected resonances are visible, with assignments as indicated in the figure. In the case of **II** there are no differences between the chemical shifts in solution vs the solid state. It might be expected, for example, that sites 4 and 7 could appear slightly downfield of

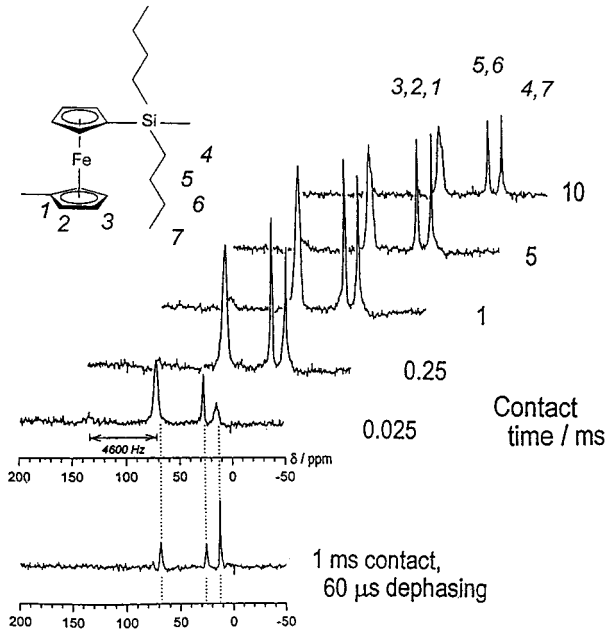

Figure 6. ^{13}C CPMAS NMR spectra at 75.5 MHz and room temperature for poly(ferrocenyl di-*n*-butylsilane) (**II**) at selected contact times; 20 Hz Lorentzian broadening has been added. The lower figure shows a dipolar dephased spectrum (60 μs, acquisition from top of first rotational echo, arbitrary phasing) used to confirm the assignments.

their values in solution, based on the γ-gauche effect and the expectation that a higher proportion of trans (anti) conformers should be present in the solid state.[40,41] Furthermore, there is no discernible splitting of the innermost (site 4) methylene resonance such as one might expect by analogy with the methyl resonance of **I**. This might be explicable on the basis of the greater main chain spacing in **II** vs **I** which would tend to reduce intermolecular interactions, thereby eliminating a major factor favoring the mixed conformation for **I**.[36]

Proton−Carbon Cross-Polarization Dynamics. The cross-polarization behavior of **I** and **II** is shown in Figure 7. A logarithmic time scale is used in order to emphasize differences in the initial build-up behavior. In general, as expected for a semicrystalline polymer, there is an initial rapid increase in intensity and a subsequent intensity decay with increasing contact time in the cross-polarization experiment.

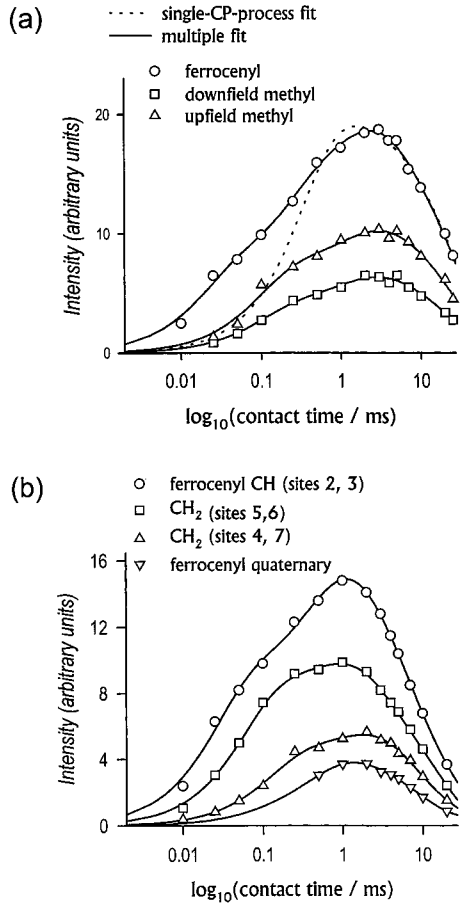

Figure 7. (a) Resonance line intensity vs the cross-polarization (CP) contact time for polymer **I**. The vertical scales are arbitrary. The methyl resonances have been arbitrarily vertically scaled for clarity. The curves are fits to eq 1 using parameters listed in Table 2. (b) Resonance line intensity vs CP contact time for polymer **II**. Alkyl intensities have been arbitrarily vertically scaled for clarity. For fitted parameters, see Table 3.

For a given carbon in a given phase, the dependence of the ^{13}C magnetization, $I(t)$, on contact time, t, is described by[23]

$$I(t)/I(0) = \lambda^{-1} f(t)$$

$$\lambda = 1 + \frac{T_{CH}}{T_{1\rho}(C)} - \frac{T_{CH}}{T_{1\rho}(H)}$$

$$f(t) = \exp\left(-\frac{t}{T_{1\rho}(H)}\right) - \exp\left[-t\left(\frac{1}{T_{CH}} + \frac{1}{T_{1\rho}(C)}\right)\right] \quad (1)$$

where T_{CH} is the characteristic cross-polarization time between protons and carbons, and $T_{1\rho}(H)$ and $T_{1\rho}(C)$ are the time constants for decay of the proton and carbon spin-locked magnetizations, respectively. $T_{1\rho}(H)$ is measured from the slope of the signal decay at long contact times. Details for **I** and **II** are provided in Tables 2 and 3, respectively. The quantity $[1/T_{CH} + 1/T_{1\rho}(C)]$ may then be evaluated from the initial rate of buildup of magnetization at short contact times. Details are provided in Tables 2 and 3. $T_{1\rho}(C)$ must be measured in a separate experiment. Without this information a proper value for the scaling quantity λ cannot be calculated, and true intensities (i.e., spin counts) cannot be obtained from measured intensities. Therefore, we have compared only relative values of $I(0)$ obtained from the value of $I(t)$ extrapolated to $t = 0$ from the $T_{1\rho}(H)$ decay for different carbon sites in **I** and **II**, as detailed in Tables 2 and 3.

Table 2. Cross-Polarization Parameters for Poly(ferrocenyl dimethylsilane) (Polymer I) from Fitting the Data of Figure 7a to Eq 1

	chemical shift		
parameter	73 ppm[a]	2.8 ppm[b]	−1.6 ppm[c]
Crystalline Phase			
$T_{1\rho}(H)$ (ms)	27.4[d]	27.4	27.4
T_{CH} (μs)[e]	18.7	94.2	94.8
% total	38	50	58
Amorphous Phase ($T > T_g$[f])			
$T_{1\rho}(H)$ (ms)	27.0	21.9	27.6
T_{CH} (μs)[e]	490	1134	1276
% total	62	50	42

[a] Cyclopentadienyls, includes the intensities of the first-order spinning sidebands. [b] Downfield methyl. [c] Upfield methyl. [d] Fits were obtained with a fixed value of $T_{1\rho}^H$ (long) for all sites. [e] Strictly equal to $[1/T_{CH} + 1/T_{1\rho}(C)]^{-1}$ since no separate measurement was made for $1/T_{1\rho}(C)$. [f] NMR T_g; for mechanical T_g see Table 1.

Table 3. Cross-Polarization Parameters for Poly(ferrocenyl di-*n*-butylsilane) (Polymer II) from Fitting the Data of Figure 7b to Eq 1

	chemical shift			
parameter	73 ppm[a]	71 ppm[b]	28 ppm[c]	15 ppm[d]
Crystalline Phase				
$T_{1\rho}(H)$ (ms)	18.6[e]	18.6	18.6	18.6
T_{CH} (μs)[f]	26.8	305.2	53.5	121.3
% total	52	50	68	61
Amorphous Phase ($T > T_g$[g])				
$T_{1\rho}(H)$ (ms)	5.7	6.1	3.1	4.9
T_{CH} (μs)[f]	463	519	491	1346
% total	48	50	32	39

[a] Carbons 2 and 3. [b] Carbon 1. [c] Carbons 5 and 6. [d] Carbons 4 and 7. [e] Fits were obtained with a fixed value of $T_{1\rho}^H$ (long). [f] Strictly equal to $[1/T_{CH} + 1/T_{1\rho}(C)]^{-1}$ since no separate measurement was made for $1/T_{1\rho}(C)$. [g] NMR T_g; for mechanical T_g see Table 1.

Satisfactory fits to the contact time-dependent intensities in Figure 7 using eq 1 are only obtained upon assuming that at least two phases coexisted in the polymer samples, each with unique time constants as detailed in Tables 2 and 3. Assuming a single phase yields a poor fit to the data. The time constants differ markedly for the different components and are consistent with coexisting crystalline and glassy amorphous regions within the samples.

Specifically, the cross-polarized intensity growth and decay processes are mediated through dipolar interactions. The various time constants are influenced, therefore, by motions tending to reduce the effective dipolar interaction. This provides a basis for morphological distinction in polymers.[11c] Other factors being constant, more rigid regions, such as those which are crystalline or rigid glassy, cross-polarize rapidly (short T_{CH}) and decay slowly (long $T_{1\rho}(H)$). Conversely, more mobile regions, such as those which are amorphous, exhibit longer T_{CH} and shorter $T_{1\rho}(H)$.

The necessity of using multiple components to fit the cross-polarized intensities is particularly evident at short contact times (up to ca. 200 μs). Here, only those ^1H spins in the near vicinity of the ^{13}C spin under scrutiny have sufficiently large dipolar couplings to contribute magnetization so rapidly. Consequently, the transfer process, in this short amount of time, is

dominated by the dipolar coupling between the carbon in question and its attached protons. Hence, this tends to select protonated carbons in crystalline regions of the sample. Moreover, complicating issues such as the effect of resonance offset on the maximum achievable signal[42] or the advent of spinning sidebands in the matching condition when spinning rates are comparable to the local dipolar field of the protons[27] are avoided. Furthermore, presupposing that $T_{CH} < T_{1\rho}(C) \ll T_{1\rho}(H)$, these data reflect predominantly the influence of T_{CH}.

As shown in Table 2, values of T_{CH} are longer in the amorphous vs the crystalline component, for both the cyclopentadienyl and methyl carbons of **I**, in keeping with the expected greater mobility within an amorphous phase. Comparing the cyclopentadienyl vs methyl carbons of **I** demonstrates that the cyclopentadienyl ring carbons cross-polarize rapidly with their attached proton, while the methyl carbons do so more slowly, in keeping with the reduced proton−carbon dipolar interaction produced by methyl rotations. However, only in the crystalline phase do cross-polarization rates for the cyclopentadienyl ring carbons approach the maximum expected for essentially rigid structures.[17c]

The T_{CH} values for the methyl carbons of **I** in the crystalline phase are somewhat longer than expected of methyl groups that are subject to methyl rotation only,[43] without accompanying additional freedom. It is tempting, therefore, to equate this with the presence of main chain motion. However, the weaker dipolar interaction between methyl protons and carbons means that the contribution of neighboring protons to the cross-polarization process becomes an issue. Since these contributions are not easy to estimate, drawing conclusions becomes problematic.

Values of $T_{1\rho}(H)$ are similar at all sites in **I**, indicating that spin diffusion is sufficiently rapid as to create a common proton magnetization pool. This implies that even the amorphous phase is still relatively rigid.

Turning to the T_{CH} values for **II**, as listed in Table 3, one observes, again, that cross-polarization occurs more quickly in crystalline vs amorphous regions. The cyclopentadienyl ring carbons exhibit cross-polarization rates suggestive of an essentially rigid environment, although somewhat more mobile than in **I**. This implies that **II** may be predisposed to disorder of the main chain.

The T_{CH} values of the methylene units of **II** are much longer than would be expected of rigid CH_2 units,[17,43] which are typically on the order of 20 μs. Evidently, the side chains of **II** are in a state of considerable dynamic disorder, with rates of motion exceeding $1/T_{CH}^{rigid}$, i.e., on the order of 10^5 Hz or faster.

As for values of $T_{1\rho}(H)$, all carbons in the crystalline phase display similar values. However, in the amorphous phase significant differences between carbons begin to appear, suggesting that rates of motion have increased sufficiently to somewhat "decouple" the different proton spin pools.

Discussion

In this section, we consider the relevance of the room-temperature NMR measurements to the transition at ca. 127 °C which is observed in the DSC trace of **II**. Cross-polarization measurements indicate that the cyclopentadienyl carbons in both **I** and **II** are rigid in the crystalline lattice. However, there was an indication that the cyclopentadienyl methines of **II** are slightly more mobile than their counterparts in **I**, suggesting that the main chains of **II** may be somewhat more mobile. The side chains of **II** were found to be very disordered, so that the overall picture of the conformational conditions in the lattice of **II** is that of fairly stable main chains separated by loose side chains. By contrast, the main chains of **I** are rigid and stable, and although the methyl groups may undergo some librational motions (in addition to the normal methyl rotation process), they are not large enough to isolate main chains from one another as with *n*-butyl side chains. Consistent with this is the chemical shift information: an unsymmetrical doublet is seen for the ^{13}C signals from the methyls of **I**, attributable to either a mixed conformation or a mixture of crystalline phases. The former situation occurs in the associated pentamer and was explained by Barlow et al.[36] in terms of an intra- and intermolecular dispersive force effect wherein the large positive partial charge at the iron centers attracts neighboring cyclopentadienyl rings, producing a network of stabilizing forces. For **II**, no such difference can be discerned between solution and solid-state ^{13}C NMR spectra, suggesting that its crystal lattice is not as tightly packed.

Given that the structure of **II** can be envisaged as stable main chains surrounded by mobile alkyl chains, it is perhaps not too surprising that a transition appears to occur at higher temperature. Possibly the higher temperature is required to give sufficient thermal activation for a lamellar thickening process. Such a process has already been established for submelting transitions exhibited by a different polymorph of **I.** The advent of a "rotator" or "conformationally disordered" (condis) phase can be reasonably anticipated with a lamellar thickening transition. The connection was noted by Wunderlich et al. for ultrahigh-molecular-weight polyethylene,[9a] and the phenomenon of the condis phase has been observed in a range of polymer types.[9a] These include polysilanes[9b−e] with di-*n*-alkyl substituents: for example, the side chains in poly(di-*n*-hexyl)silane were shown to be disordered, but still with a preferential disposition normal to the main chain.[9d] At higher temperatures, dynamic conformational disorder of the main chain arose. An analogous situation with the poly(ferrocenylsilanes), particularly **II**, would be interchange of conformational states in the main chain at the higher transition temperature (ca. 127 °C).

Conclusions

Solid-state ^{13}C NMR of two members of the poly(ferrocenyl dialkylsilane) family reveal significant differences in crystalline conformation and motions which arise when the *n*-alkyl side chain is increased in length, from methyl to *n*-butyl. Acquiring spectra from a wide range of cross-polarization times allows a further distinction to be made, in terms of morphological phases, of both the initial CP buildup and subsequent spin−lattice $T_{1\rho}(H)$ decay. The main chains of both polymers are fairly rigid in their crystalline lattices, although some libration of ferrocenyl groups is possible in the case of **II**. The side chains of **II** are, however, dynamically disordered.

On the basis of the looser packing of the crystalline lattice of **II** compared to **I**, as manifest in both chemical shift values and short contact time cross-polarization behavior, as well as previous investigations which

revealed lamellar thickening processes in a different polymorph of **I**, it is concluded that at room temperature the main chain conformation and side chain disorder of **II** may enable it to undergo a *condis* transition at higher temperatures. This would explain the small, additional endotherm which occurs just prior to complete melting. It is suggested that this can occur for the polymer as normally prepared because of the greater separation of the main chains as evident in the systematic variation in WAXS profiles according to the length of the short side chains. An NMR investigation into the exact nature of the crystalline transition and the possible involvement of the amorphous regions would seem appropriate.

Acknowledgment. J.R., G.J.V., and I.M. acknowledge the Natural Sciences and Engineering Research Council (NSERC) of Canada and the Institute of Chemical Sciences for funding. P.M.M. and I.M. thank Materials and Manufacturing Ontario (MMO) and NSERC for operating grants. K.K. thanks NSERC for a Postgraduate Scholarship. I.M. is a recipient of an Alfred P. Sloan Fellowship (1994−1998), an E.W.R. Steacie Fellowship (1997−1999), and a McLean Fellowship (University of Toronto; 1997−2003). We also thank Dr. R. Jaeger for help with the Cerius software package as well as numerous useful discussions, Drs. T. Nicholson (University of Leeds, UK) and J. Grima (University of Exeter, UK) for use of their Cerius[2] software, Dr. D. Foucher for sample preparation throughout the project, and J. Massey and R. Perry for additional supplies of the dimethyl and di-*n*-butyl polymers, respectively.

References and Notes

(1) Manners, I. *Chem. Commun.* **1999**, 857−65.
(2) Manners, I. *Chem. Br.* **1996**, *32*, 46−9.
(3) (a) Manners, I. *Angew. Chem., Int. Ed. Engl.* **1996**, *35*, 1603−1621. (b) Manners, I. *Adv. Organomet. Chem.* **1995**, *37*, 131−68.
(4) (a) Foucher, D. A.; Tang, B. Z.; Manners, I. *J. Am. Chem. Soc.* **1992**, *114*, 6246−8. (b) Foucher, D. A.; Ziembinski, R.; Tang, B.-Z.; Macdonald, P. M.; Massey, J.; Jaeger, C. R.; Vancso, G. J.; Manners, I. *Macromolecules* **1993**, *26*, 2878−84. (c) Foucher, D. A.; Ziembinski, R.; Petersen, R.; Pudelski, J. K.; Edwards, M.; Ni, Y.; Massey, J.; Jaeger, C. R.; Vancso, G. J.; Manners, I. *Macromolecules* **1994**, *27*, 3992−9. (d) Manners, I. *Adv. Mater.* **1994**, *6*, 68. (e) Pudelski, J. K.; Rulkens, R.; Foucher, D. A.; Lough, A. J.; Macdonald, P. M.; Manners, I. *Macromolecules* **1995**, *28*, 7301−8.
(5) (a) Rulkens, R.; Lough, A. J.; Manners, I. *J. Am. Chem. Soc.* **1994**, *116*, 797−8. (b) Rulkens, R.; Perry, R.; Lough, A. J.; Manners, I.; Lovelace, S. R.; Grant, C.; Geiger, W. E. *J. Am. Chem. Soc.* **1996**, *116*, 12683−95.
(6) Shadaram, M.; Martinez, J.; Garcia, F.; Tavares, D. *Fiber Integr. Opt.* **1997**, *16*, 115−22.
(7) (a) Hymene, M.; Yassar, A.; Escorne, M.; Percheron-Guegan, A.; Garnier, F. *Adv. Mater.* **1994**, *6*, 564−8. (b) MacLachlan, M. J.; Ginzburg, M.; Coombs, N.; Coyle, T. W.; Raju, N. D.; Greedan, J. E.; Ozin, G. A.; Manners, I. *Science* **2000**, *287*, 1460−1463.
(8) Massey, J.; Power, K. N.; Manners, I.; Winnik, M. A. *J. Am. Chem. Soc.* **1998**, *120*, 9533−9540.
(9) (a) Wunderlich, B.; Möller, M.; Gerbowicz, J.; Baur, H. *Adv. Polym. Sci.* **1988**, *87*, 1. (b) Schilling, F. C.; Gomez, M. A.; Tonelli, A. E.; Bovey, F. A.; Woodward, A. E. *Macromolecules* **1987**, *20*, 2954−7. (c) Gobbi, G. C.; Fleming, W. W.; Sooriyakumaran, R.; Miller, R. D. *J. Am. Chem. Soc.* **1986**, *108*, 5624−6. (d) Lovinger, A. J.; Schilling, F. C.; Bovey, F. A.; Zeigler, J. M. *Macromolecules* **1986**, *19*, 2660−3. (e) Walsh, C. A.; Schilling, F. C.; MacGregor, R. B.; Lovinger, A. J.; Davis, D. D.; Bovey, F. A.; Zeigler, J. M. *Synth. Met.* **1989**, *28*, C559−64.
(10) Schaefer, J.; Stejskal, E. O. *Top. Carbon-13 NMR Spectrosc.* **1979**, *3*, 284−324.
(11) (a) Yannoni, C. S. *Acc. Chem. Res.* **1982**, *15*, 201−8. (b) Lyerla, J. R.; Yannoni, C. S.; Fyfe, C. A. *Acc. Chem. Res.* **1982**, *15*, 208−16. (c) Voelkel, R. *Angew. Chem., Int. Ed. Engl.* **1988**, *27*, 1468−83.
(12) McCall, D. W. *Acc. Chem. Res.* **1971**, *4*, 223−32.
(13) McBrierty, V. J.; Packer, K. J. *NMR Spectroscopy of Solid Polymers*; Cambridge University Press: Cambridge, 1993.
(14) (a) Packer, K. J.; Pope, J. M.; Yeung, P. R.; Cudby, M. E. A. *J. Polym. Sci., Polym. Phys. Ed.* **1984**, *22*, 589−616. (b) Kenwright, A. M.; Say, B. J. In *NMR Spectroscopy of Polymers*; Ibbett, R. N., Ed.; Blackie Academic and Professional (Chapman & Hall): London, 1993; Chapter 7.
(15) Spiess, H. W. *Adv. Polym. Sci.* **1985**, *66*, 23−58.
(16) Kulbaba, K.; Macdonald, P. M.; Manners, I. *Macromolecules* **1999**, *32*, 1321−1324.
(17) (a) Lauprêtre, F.; Monnerie, L.; Virlet, J. *Macromolecules* **1984**, *17*, 1397−1405. (b) Lauprêtre, F.; Noël, C.; Jenkins, W. N.; Williams, G. *Faraday Discuss. Chem. Soc.* **1985**, *79*, 191−99. (c) Lauprêtre, F. In *NMR Spectroscopy of Polymers*; Ibbett, R. N., Ed.; Blackie Academic and Professional (Chapman & Hall): London, 1993; Chapter 6.
(18) Schaefer, J.; Stejskal, E. O.; McKay, R. A.; Dixon, W. T. *Macromolecules* **1984**, *17*, 1479−89.
(19) McBrierty, V. J.; Douglass, D. C. *Phys. Rep.* **1980**, *63*, 61−147.
(20) Munowitz, M. *Coherence and NMR*; Wiley: New York, 1988, pp 146, 221.
(21) Wu, X. L.; Zilm, K. W. *J. Magn. Reson.* **1991**, *93*, 265−78.
(22) Pines, A.; Gibby, M. G.; Waugh, J. S. *J. Chem. Phys.* **1973**, *59*, 569−90.
(23) Mehring, M. *Principles of High-Resolution NMR in Solids*; Springer-Verlag: Berlin, 1983; Chapter 4.
(24) (a) Stejskal, E. O.; Schaefer, J. *J. Magn. Reson.* **1974**, *14*, 160−9. (b) Hoult, D. I.; Richards, R. E. *Proc. R. Soc. London, Ser. A* **1975**, *344*, 311−40. (c) Stejskal, E. O.; Schaefer, J. *J. Magn. Reson.* **1975**, *18*, 560−3. (d) Tegenfeldt, J.; Haeberlen, U. *J. Magn. Reson.* **1979**, *36*, 453−7.
(25) Hartmann, J. M.; Hahn, E. L. *Phys. Rev.* **1962**, *128*, 2048−53.
(26) Earl, W. L.; VanderHart, D. L. *J. Magn. Reson.* **1982**, *48*, 35−54.
(27) (a) Stejskal, E. O.; Schaefer, J.; Waugh, J. S. *J. Magn. Reson.* **1977**, *28*, 105−112. (b) Meier, B. H. *Adv. Magn. Opt. Reson.* **1994**, *18*, 1−116. (c) Wind, R. A.; Dec, S. F.; Lock, H.; Maciel, G. E. *J. Magn. Reson.* **1988**, *88*, 136−9.
(28) VanderHart, D. L.; Earl, W.; Garroway, A. N. *J. Magn. Reson.* **1981**, *44*, 361−401.
(29) Garroway, A. N.; Earl, W. L.; VanderHart, D. L. *Philos. Trans. R. Soc. London* **1981**, *A299*, 609−28.
(30) Frye, J. S.; Maciel, G. E. *J. Magn. Reson.* **1982**, *48*, 125−31.
(31) (a) Rasburn, J.; Petersen, R.; Jahr, T.; Rulkens, R.; Manners, I.; Vancso, G. J. *Chem. Mater.* **1995**, *7*, 871. (b) Lammertink, R. G. H.; Hempenius, M. A.; Manners, I.; Vancso, G. J. *Macromolecules* **1998**, *31*, 795−800. (c) Lammertink, R. G. H.; Hempenius, M. A.; Vancso, G. J. *Macromol. Chem. Phys.* **1998**, *199*, 2141−5. (d) Papkov, V. S.; Gerasimov, M. V.; Dubovik, I. I.; Sharma, S.; Dementiev, V. V.; Pannell, K. H. *Macromolecules* **2000**, *33*, 7107−15.
(32) Cerius (Cerius[2]) Molecular Simulations Inc., San Diego, CA; Cambridge, England.
(33) Alexander, L. E. *X-ray Diffraction Methods in Polymer Science*; Wiley-Interscience: New York, 1969.
(34) Berger, K.; Baullauff, M. *Mol. Cryst. Liq. Cryst.* **1988**, *157*, 109−23.
(35) Axelson, D. A. In *High-Resolution NMR Spectroscopy of Synthetic Polymers in Bulk*; Komoroski, R. A., Ed.; VCH: Deerfield Beach, FL, 1986; Chapter 5.
(36) (a) Barlow, S.; Rohl, A.; O'Hare, D. *J. Chem. Soc., Chem. Commun.* **1996**, 257−60. (b) Barlow, S.; Rohl, A. L.; Shi, S.; Freeman, C. M.; O'Hare, D. *J. Am. Chem. Soc.* **1996**, *118*, 7578−92.
(37) *Organometallic Compounds*; Green, M. L. H., Ed.; (Coates, G. E., Green, M. L. H., Wade, K., Series Eds.); Chapman & Hall: London, 1968; Vol. 2, p 142.
(38) (a) Haigh, C. W.; Mallion, R. B. *Prog. NMR Spectrosc.* **1979**, *13*, 303. (b) Bovey, F. A.; Jelinski, L. W.; Mirau, P. A. *Nuclear Magnetic Resonance Spectroscopy*, 2nd ed.; AT&T: San Diego, 1988; p 110. (c) Günther, H. *NMR Spectroscopy (An Introduction): Principles, Concepts and Applications in Chemistry*; John Wiley: New York, 1995; Appendix.
(39) Papkov, V. S.; Gerasimov, M. V.; Dubovik, I. I.; Sharma, S.; Dementiev, V. V.; Pannell, K. H. *Macromolecules* **2000**, *33*, 7107−15.

(40) (a) Schilling, F. C.; Tonelli, A. E. *Acc. Chem. Res.* 1**981**, *14*, 233−8. (b) Tonelli, A. E. *NMR and Polymer Microstructure: The Conformational Connection*; VCH: New York, 1989. (c) Tonelli, A. E. In *NMR Spectroscopy of Polymers*; Ibbett, R. N., Ed.; Blackie Academic and Professional (Chapman & Hall): London, 1993; Chapter 5.

(41) The γ-gauche effect describes the relative chemical shifts of *anti* ("*trans*") and *syn* ("*gauche*") conformations of vinyl polymer chains. When a ^{13}C spin is in a *gauche* arrangement with another ^{13}C spin three bonds away (i.e., dihedral angle of $\pm 60°$), both have chemical shifts several ppm upfield from the *trans* situation. The actual difference depends on the chemical structure (e.g., polyethylene, polypropylene, poly(vinyl chloride)). In solution or in the melt, where there is rapid conformational interchange, the observed shift will be intermediate between the extremes of *trans*-only or *gauche*-only, being a weighted average according to the relative probabilities of each conformation.

(42) (a) Levitt, M. H.; Suter, D.; Ernst, R. R. *J. Chem. Phys.* **1986**, *84*, 4243−55. (b) Demco, D. E.; Tegenfeldt, J.; Waugh, J. S. *Phys. Rev.* **1975**, *B11*, 4133−51. (c) Muller, L.; Ernst, R. R. *Mol. Phys.* **1979**, *38*, 963−92. (d) Bax, A.; Hawkins, B. L.; Maciel, G. E. *J. Magn. Reson.* **1984**, *59*, 530−9.

(43) Reinheimer, P.; Hirschinger, J.; Gilard, P.; Goetz, N. *Magn. Reson. Chem.* **1997**, *35*, 757−64 and references therein.

MA0006934